J|A|C|S
ARTICLES
Published on Web 07/06/2006

Photoelectrochemical Immunosensor for Label-Free Detection and Quantification of Anti-cholera Toxin Antibody

Naoufel Haddour, Jérôme Chauvin, Chantal Gondran, and Serge Cosnier*

Contribution from the Laboratoire d'Electrochimie Organique et de Photochimie Rédox (CNRS UMR 5630), Institut de Chimie Moléculaire de Grenoble FR CNRS 2607, Université Joseph Fourier, BP 53, 38041 Grenoble Cedex 9, France

Received April 19, 2006; E-mail: serge.cosnier@ujf-grenoble.fr

Abstract: We demonstrate herein a newly developed photoelectrochemical immunosensor for the determination of anti-cholera toxin antibody by using a photosensitive biotinylated polypyrrole film. The latter was generated by electro-oxidation of a biotinylated tris(bipyridyl) ruthenium(II) complex bearing pyrrole groups. The photoexcitation of this modified electrode potentiostated at 0.5 V vs SCE, in the presence of an oxidative quencher, pentaaminechloro cobalt(III) chloride (15 mM), led to a cathodic photocurrent. As a result of the affinity interactions, a layer of biotinylated cholera toxin was firmly bound to the functionalized polypyrrole film via avidin bridges. The resulting modified electrodes were tested as immunosensors for the detection of the corresponding antibody from 0 to 200 μg mL^{-1}. The antibody concentration was measured through the decrease in photocurrent intensity resulting from its specific binding onto the polymeric coating, the detection limit being 0.5 μg mL^{-1}.

Introduction

Affinity biosensors such as receptor sensors, immunosensors, and DNA sensors are analytical tools exploiting specific interactions between carbohydrates and proteins, antibodies and antigens, and nucleic acid recognition processes. This group of biosensor has received considerable attention into an ever expanding application field.[1−5] There are two key steps in the development of affinity sensors: the fabrication of the recognition layer at the transducer surface and the transduction of the related recognition event. Most of the affinity sensors developed so far rely on the indirect optical detection. Effectively, fluorescence, bioluminescence, and electrochemiluminescence are highly sensitive standard methods for detection of the duplex formation or immunoreaction by marking the target with either a fluorescent dye or an enzyme as in enzyme-linked immunoassay (ELISA).[6−11] However, these techniques necessitate an additional labeling step of the target involving incubation and washing steps that increase markedly the analysis time and its cost. Moreover, sufficiently high spatial resolution for high throughput diagnostic applications requires a complex, non-miniaturized, and costly confocal system that considerably limits the widespread use of optical readouts. Increased attention has been thus given to photoelectrochemical procedures with electronic detection that are simpler in instrumentation and easier to miniaturize than conventional optical methods. In particular, Guo et al. reported recently the first quantitative photoelectrochemical detection of biotin via its labeling by a ruthenium(II) tris(bipyridyl) complex as photosensitizer.[12] More recently, ruthenium tris(bipyridine) was immobilized on an electrode surface to perform the photoelectrochemical detection of DNA via the oxidation of the guanine bases by the photogenerated Ru(III) species, thus opening attractive perspectives for the development of photoelectrochemical DNA sensors.[13]

With the aim of developing a new label-free photoelectrochemical detection concept for immunosensors, we report herein the design and characterization of a novel ruthenium(II) tris-(bipyridyl) polymer film allowing both the immobilization of proteins and the direct transduction of immunoreaction via the evolution of its photoelectrochemical properties. The quality of both the photosensitive layer and the immobilized antigen layer, at which the molecular recognition process takes place, is of extreme importance in the achievement of suitable immunosensor sensitivity. Consequently, the ruthenium complex was functionalized by electropolymerizable pyrrole groups and biotin as affinity binding groups (Figure 1). The electrochemical polymerization of organic polymers, indeed, is one of the few procedures of surface functionalization with molecular reagents that allows the reproducible and accurate functionalization of

(1) Wang, J. *Anal. Chim. Acta* **2002**, *469*, 63.
(2) Gooding, J. J. *Electroanalysis* **2002**, *14*, 366.
(3) Tiefenauer, L.; Ros, R. *Colloids Surf., B* **2002**, *23*, 95.
(4) Katz, E.; Willner, I. *Electroanalysis* **2003**, *15*, 913.
(5) Jelinek, R.; Kolusheva, S. *Chem. Rev.* **2004**, *104*, 5987.
(6) Ali, M. F.; Kirby, R.; Goodey, A. P.; Rodriguez, M. D.; Ellington, A. D.; Neikirk, D. P.; McDevitt, J. T. *Anal. Chem.* **2003**, *75*, 4732.
(7) Wang, J. *Nucleic Acids Res.* **2000**, *28*, 3011.
(8) Lui, X.; Tan, W. *Anal. Chem.* **1999**, *71*, 5054.
(9) Yakovleva, J.; Davidsson, R.; Bengtsson, M.; Laurell, T.; Emnéus, J. *Biosens. Bioelectron.* **2003**, *19*, 21.
(10) Herrmann, S.; Leshem, B.; Landes, S.; Rager-Zisman, B.; Marks, R. S. *Talanta* **2005**, *66*, 6.
(11) Endo, T.; Okuyama, A.; Matsubara, Y.; Nishi, K.; Kobayashi, M.; Yamamura, S.; Morita, Y.; Takamura, Y.; Mizukami, H.; Tamiya, E. *Anal. Chim. Acta* **2005**, *531*, 7.
(12) Dong, D.; Zheng, D.; Wang, F.-Q.; Yang, X.-Q.; Wang, N.; Li, Y.-G.; Guo, L.-H.; Cheng, J. *Anal. Chem.* **2004**, *76*, 499.
(13) Liang, M.; Liu, S.; Wei, M.; Guo, L.-H. *Anal. Chem.* **2006**, *78*, 621.

10.1021/ja062729z CCC: $33.50

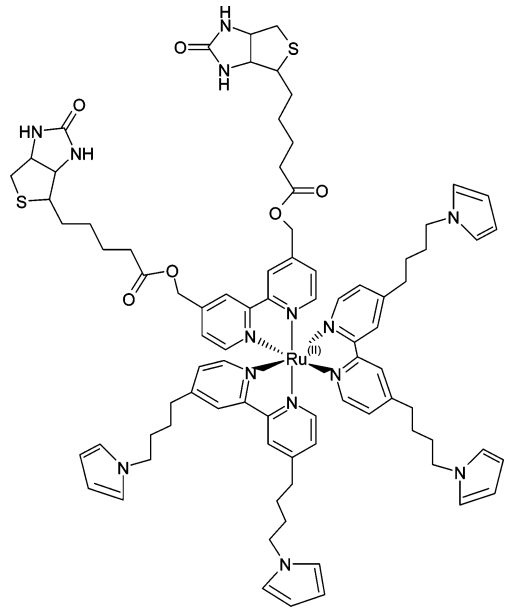

Figure 1. Structure of the $[Ru(L_2)_2(L_1)]^{2+}$ complex.

conductive surfaces.[14−16] In addition, the quality of the electrogenerated polymer films (absence of manufacturing defects, chemical stability, and storage stability) constitutes an attractive advantage for the regularity at the molecular level of additional functionalization of the electrode via the polymer film. In particular, the combination of electropolymerized films with high affinity avidin−biotin interactions provided an efficient method for biomolecule immobilization with a high degree of control over the molecular architecture.[17−19] The latter was based on the electrogeneration of biotinylated films that allow the subsequent attachment of biotinylated molecules (enzymes, antibodies, bacteria) through the formation of avidin bridges. Moreover, the avidin−biotin immobilization procedure involves solely a single attachment point of the biomolecules, facilitating thus recognition phenomenon such as immunoreaction.

Photochemical measurements were carried out to examine the avidin-binding properties of a biotin-labeled ruthenium(II) tris(bipyridyl) complex functionalized by four pyrrole groups $[Ru(L_2)_2(L_1)]^{2+}$ and those of the corresponding electropolymerized film. The photophysical and electrochemical properties of the polymer film were then investigated to design a photoelectrochemical immunosensor for the direct label-free determination of anti-cholera toxin antibody.

Experimental Section

Reagents. Avidin (Av, A9390, from egg white, 89% of protein by UV absorbance), bovine serum albumin (BSA, A4503, fraction V), cholera toxin B subunit, biotin labeled (CT, C9972, lyophilized powder containing approximately 40% protein), anti-cholera toxin antibody (anti-CT, C3062, from rabbit, purified toxin from vibrio cholerae), avidin alkaline phosphatase labeled (AP, 410 U mg^{-1}), and polyoxyethylene-sorbitan monolaurate (Tween 20, P7949) were purchased from Sigma.

4,4′-Bis(biotin)-2,2′-bipyridine (L_1) was synthesized as previously reported.[20] Biotin (488 mg, 2 mM), dicyclohexylcarbodiimide (412 mg, 2 mM), and NHS (230 mg, 2 mM) in DMF (20 mL) were stirred at 80 °C under argon for 3 h and cooled to room temperature. To this solution were added 4,4′-bis(hydroxymethyl)-2,2′-bipyridine (151 mg, 0.7 mM) and 4-(dimethylamino) pyridine (61 mg, 0.5 mM). The reaction mixture was stirred at 60 °C for 60 h and then cooled to room temperature and filtered. The organic solvent was removed under vacuum, and the residue crystallized from AcOEt. Yield: 668 mg (48%). ^{1}H NMR (DMSO, 250 MHz): δ (ppm) = 1.20 (m, 4H), 1.24 (m, 4H), 1.46 (m, 4H), 2.00 (t, 4H), 2.74 (d, 2H), 2.80 (d, 2H), 3.06 (m, 2H), 4.09 (m, 2H), 4.26 (m, 4H), 5.24 (s, 4H), 6.37 (s, 2H), 6.45 (s, 2H), 7.44 (d, 2H), 8.36 (s2H), 8.69 (d, 2H). FAB/MS(NBA): m/z = 669 [MH^+].

4,4′-Bis(4-pyrrole-1-butyl)-2,2′-bipyridine (L_2). BuLi (9.6 mL) was added to a solution of diisopropylamine (3.3 mL) in THF (15 mL), and the resulting mixture was stirred for 15 min. Next, 2.1 g of 4,4′-dimethyl-2,2′bipyridine in THF (80 mL) was added from a dropping funnel, and the reaction mixture was stirred for 2 h at room temperature. 1-(3-Bromopropyl)-pyrrole (4.5 g) in THF (40 mL) was added, and stirring was continued for 1 h. The reaction was stopped by addition of water, and then the mixture was extracted with CH_2Cl_2. The solvent was evaporated, and the residue was purified by chromatography (silica, eluent: CH_2Cl_2/CH_3OH [9/1]) providing a white solid. Yield: 1.8 g (40%). ^{1}H NMR (250 MHz/$CDCl_3$): δ (ppm) = 1.67 (m, 4H), 1.83 (m, 4H), 2.68 (t, 4H), 3.90 (t, 4H), 6.12 (s, 4H), 6.62 (s, 4H), 7.10 (d, 2H), 8.21 (s, 2H), 8.56 (d, 2H). FAB/MS(NBA): m/z = 399 [MH^+].

$[Ru(L_2)_2(L_1)]^{2+}$ was prepared as previously described by refluxing for 4 h in ethanol (10 mL) an equimolar amount of L_1 (4,4′-bis(biotin)-2,2′bipyridine) (50 mg, 0.075 mM) and $Ru(II)(L_2)_2Cl_2$ (73 mg, 0.075 mM).[21] The latter was synthesized from the reaction of 4,4′-bis(4-pyrrole-1-butyl)-2,2′-bipyridine (L_2) with $Ru(III)Cl_3$. After cooling to room temperature, the reaction mixture was filtered, and the ruthenium complex was precipitated by adding an aqueous solution of potassium hexafluorophosphate (290 mg in 25 mL). The latter was purified by chromatography (alumina, eluent: CH_3CN/CH_3OH (7/3) + 10^{-3} M KPF_6) and then crystallized from acetone/diethyl ether. Yield: 80 mg (65%).

^{1}H NMR (250 MHz/CD_3CN) data for the ruthenium complex: δ (ppm) = 1.18 (m, 4H), 1.22 (m, 4H), 1.45 (m, 4H), 1.75 (m, 4H), 1.90 (m, 4H), 2.03 (t, 4H), 2.76 (m, 4H), 2.80 (d, 2H), 2.85 (d, 2H), 3.05 (m, 2H), 3.89 (t, 4H), 4.16 (m, 2H), 4.34 (m, 4H), 5.24 (s, 4H), 5.37 (s, 2H), 5.43 (s, 2H), 6.05 (s, 4H), 6.62 (s, 4H), 7.16 (m, 4H), 7.32 (d, 2H), 7.46 (m, 4H), 7.64 (d, 2H), 8.23 (s, 4H), 8.43 (s, 2H). UV−vis (CH_3CN) λ_{max}/nm = 460 (14 200). EI-MS: m/z = 1710 [M − PF_6], 1565 [M − 2PF_6]. All other reagents were of analytical grade.

Physical Measurements and Instrumentation. UV−vis spectra were obtained using a Cary 1 absorption spectrophotometer on 1 cm path length quartz cells. The steady-state emission spectra were recorded on a photon Technology International (PTI) SE-900M spectrofluorimeter. Emission quantum yield ϕ_L values were determined at 25 °C in deoxygenated solutions with a solution of $[Ru(bpy)_3]^{2+}$ as a standard (ϕ_L^{ref} = 0.062 in CH_3CN[22] and ϕ_L^{ref} = 0.042 in H_2O[23]) according to eq 1:

$$\phi_L = \frac{I_L^S}{I_L^{ref}} \frac{(1 - 10^{-OD^{ref}})}{(1 - 10^{-OD})} \phi_L^{ref} \quad (1)$$

where I_L^S, the emission intensity, was calculated from the spectrum

(14) Gerard, M.; Chaubey, A.; Malhotra, B. D. *Biosens. Bioelectron.* **2002**, *17*, 345.
(15) Schuhmann, W. *Rev. Mol. Biotech.* **2002**, *82*, 425.
(16) Cosnier, S. *Electroanalysis* **2005**, *17*, 1701.
(17) Cosnier, S.; Galland, B.; Gondran, C.; Le Pellec, A. *Electroanalysis* **1998**, *10*, 808.
(18) Yang, S. T.; Witkowski, A.; Hutchins, R. S.; Scott, D. L.; Bachas, L. G. *Electroanalysis* **1998**, *10*, 58.
(19) Torres-Rodriguez, L. M.; Roget, A.; Billon, M.; Livache, T.; Bidan, G. *Chem. Commun.* **1998**, 1993.
(20) Haddour, N.; Cosnier, S.; Gondran, C. *Chem. Commun.* **2004**, 324.
(21) Haddour, N.; Gondran, C.; Cosnier, S. *Chem. Commun.* **2004**, 2472.
(22) Juris, A.; Balzani, V.; Barigelleti, F.; Campagna, S.; Belser, P.; Von Zelewsky, A. *Coord. Chem. Rev.* **1988**, *84*, 85.
(23) Nafie, L. A.; Cheng, J. C.; Stephens, P. J. *J. Am. Chem. Soc.* **1975**, *97*, 3843.

area, and OD represents the optical density at the excitation wavelength (454 nm). The superscripts "S" and "ref" refer, respectively, to the sample and to the standard.

The luminescence lifetime of the complexes was recorded at 25 °C in a deoxygenated solution of acetonitrile or water after irradiation at $\lambda = 337$ nm with a 4 ns pulsed N_2 laser (spectra physics 337-201) and recorded, in a conventional T geometry, at $\lambda = 600$ nm using a monochromator and a photomultiplicator tube (Hammamatsu R 928) coupled with an ultrafast oscilloscope (Tektronix TDS 520 A). The emission properties of the film were analyzed with an angle of 30° between the excitation direction and the normal of the film surface.

Electrochemical investigations were performed with an EG&G Princeton Applied Research 273A potentiostat in conjunction with a Kipp and Zonen BD90 XY/t recorder. The electropolymerization of $[Ru(L_2)_2(L_1)]^{2+}$ complex and the electrochemical characterization of the resulting functionalized polypyrrole films (poly Ru) were run at room temperature under an argon atmosphere in a conventional three-electrode cell. CH_3CN (Rathburn, HPLC grade) was used as received. Ag/Ag^+ 10 mM in CH_3CN containing 0.1 M tetrabutylammonium perchlorate (TBAP) as supporting electrolyte and a saturated calomel electrode (SCE) were used as reference electrode in CH_3CN and 0.1 M acetate buffer, respectively. The working electrodes were platinum or glassy carbon disks (diameter 5 mm) polished with 1 μm diamond paste.

Photoelectrochemical measurements were performed by irradiation in the 400−800 nm region with a 100 W tungsten lamp (Oriel 66184) on modified electrodes in 0.1 M acetate buffer (pH 5) in the presence of pentaaminechloro cobalt(III) chloride (Co(III)) as oxidative quencher, the electrodes being potentiostated at 0.5 V/SCE. The cathodic photocurrent was recorded with X/t recorder.

Luminescence Titrations. In a typical procedure, aliquots of an aqueous avidin solution (5 μL, 0.5 mM) were added cumulatively to an aqueous deoxygenated solution of $[Ru(L_2)_2(L_1)]^{2+}$ (2 mL, 17 μM) at 20 min intervals. The emission spectrum of the resulting aqueous mixture was continuously measured.

Enzyme Electrode Preparation. The specific binding of enzyme to the polymerized biotin sites was performed by spreading 20 μL of avidin labeled alkaline phosphatase (AP) (0.5 mg mL^{-1}) for 20 min on the poly Ru electrode (Pt, diameter 5 mm). The resulting electrode was carefully washed under stirring with 0.1 M Tris buffer (pH 8) to remove the nonspecifically bound AP molecules.

Immunoassay Design. The biotinylated polypyrrole films ($\Gamma = 2.3 \times 10^{-8}$ mol cm^{-2}) were made, at room temperature under an argon atmosphere, by controlled potential oxidation at 0.9 V of $[Ru(L_2)_2(L_1)]^{2+}$ (1 mM) in CH_3CN + 0.1 M TBAP. The successive steps carried out for the immunosensor construction on the poly Ru films and the subsequent antibody detection are the following. A blocking solution was used to prevent the nonspecific binding of avidin as well as the simple adsorption of antigen and antibody onto the electropolymerized films. This solution, composed of 5 % (w/v) bovine serum albumin (BSA) and 0.5 % (v/v) Tween 20 in 0.1 M phosphate buffer (pH 7), was spread on the electrode and left for 15 min. The electrodes were then carefully washed several times with 0.1 M phosphate buffer. A drop (20 μL) of avidin (0.5 mg mL^{-1}) dissolved in 0.1 M phosphate buffer containing BSA (1 mg mL^{-1}) was then incubated for 30 min with the biotinylated films. After being rinsed with phosphate buffer, the resulting modified electrodes were incubated for 20 min with 20 μL of biotinylated cholera toxin B subunit (CT, 0.5 mg mL^{-1}) dissolved in phosphate buffer containing BSA. The resulting electrodes were rinsed and washed once with phosphate buffer for 10 min. The analyte, anti-cholera toxin B subunit (anti-CT) antibody at concentrations ranging from 0 to 200 μg mL^{-1}, was then spread on the resulting immunosensor and incubated for 20 min.

Table 1. MLCT Absorption Band Maxima (λ_{abs}), Luminescence Maxima (λ_{em}), Lifetime (λ), and Emission Quantum Yield (ϕ_L) for Ru(II) Complexes at 298 K

Ru(II) complex	λ_{abs} (nm)	λ_{em} (nm)	τ (ns)	ϕ_L
$[Ru(bpy)_3]^{2+}$	451[a]	604[a]	990[a] [17]	0.062[a] [17]
	423[b]	605[b]	600[b] [18]	0.042[b] [18]
$[Ru(L_2)_2(L_1)]^{2+}$	460[a]	637[a]	843[a]	0.034[a]
	432[b]	633[b]	420[b]	0.010[b]

[a] In deoxygenated CH_3CN. [b] In deoxygenated H_2O.

Result and Discussion

With the aim to develop a label-free photoelectrochemical immunosensor, we have investigated the affinity properties of the biotinylated ruthenium complex as well as its photophysical properties under the monomer and polymerized forms.

Photophysical Properties. The photophysical data of the $[Ru(L_2)_2(L_1)]^{2+}$ complex and those of the parent $[Ru(bpy)_3]^{2+}$ complex in CH_3CN and H_2O are summarized in Table 1. As expected, the electronic absorption spectra of $[Ru(L_2)_2(L_1)]^{2+}$ complex and $[Ru(bpy)_3]^{2+}$ are similar (Figure 2A). The absorption bands in the visible region (400−450 nm) are assigned to metal-to-ligand charge-transfer (^{1}MLCT) transitions [dπ (Ru) $\rightarrow \pi^*$ (bpy ligands)]. In addition, more intense bands at 250−300 nm were assigned to intra-ligand transitions [($\pi \rightarrow \pi^*$) (bpy ligands)]. These absorbances and assignments are consistent with a number of related complexes in the literature.[24−26]

The emission spectra of $[Ru(L_2)_2(L_1)]^{2+}$ and $[Ru(bpy)_3]^{2+}$ complexes upon excitation of the MLCT band at 450 nm in CH_3CN at 298 K are shown in Figure 2B. The emission maximum of the $[Ru(L_2)_2(L_1)]^{2+}$ complex occurs at 637 and 633 nm in CH_3CN and H_2O, respectively. The biotin and alkylpyrrole substitutions on the 4,4′-position of the bipyridyl ligands induce only slight modification of adsorption and emission spectra versus those of the reference $[Ru(bpy)_3]^{2+}$ complex. The ^{1}MLCT absorption and ^{3}MLCT emission bands have been red-shifted from their positions in the parent complex (Table 1). However, the emission lifetimes "τ" (ns) of $[Ru(L_2)_2(L_1)]^{2+}$ complex as well as the luminescence quantum yields are lower than those of $[Ru(bpy)_3]^{2+}$ under similar conditions. This may be ascribed to a quenching process induced by the interaction between excited ruthenium centers and biotin or pyrrole groups.

Avidin−Ru Complex Association. Among the conventional procedures of biomolecule immobilization, the strong affinity interactions between the glycoprotein avidin and four biotins, a vitamin (association constant $K_a = 10^{15}$ M^{-1}), have been extensively used.[27] The anchoring of the protein or oligonucleotide monolayer was thus performed by the simple formation of avidin bridges between biotinylated surfaces and biotinylated biomolecules. Therefore, the binding properties of the biotinylated ruthenium complex to avidin were first examined by luminescence titration. A solution of $[Ru(L_2)_2(L_1)]^{2+}$ was titrated with avidin and compared to a control titration with the parent $[Ru(bpy)_3]^{2+}$ complex. The addition of avidin to a $[Ru(L_2)_2(L_1)]^{2+}$ solution led to an increase of the emission at 637 nm, whereas no detectable change in luminescence intensity was

(24) McCafferty, D. G.; Wall, C. G.; Meyer, T. J. *J. Am. Chem. Soc*. **1993**, *115*, 1993.
(25) Kalyanasundaram, K. *Coord. Chem. Rev.* **1982**, *46*, 159.
(26) Juris, A.; Balzani, V.; Barigelletti, F.; Campagna, S.; Belser, P.; von Zelewsky, A. *Coord. Chem. Rev.* **1982**, *46*, 159.
(27) Wilchek, M.; Bayer, E. A. *Anal. Biochem.* **1988**, *171*, 1.

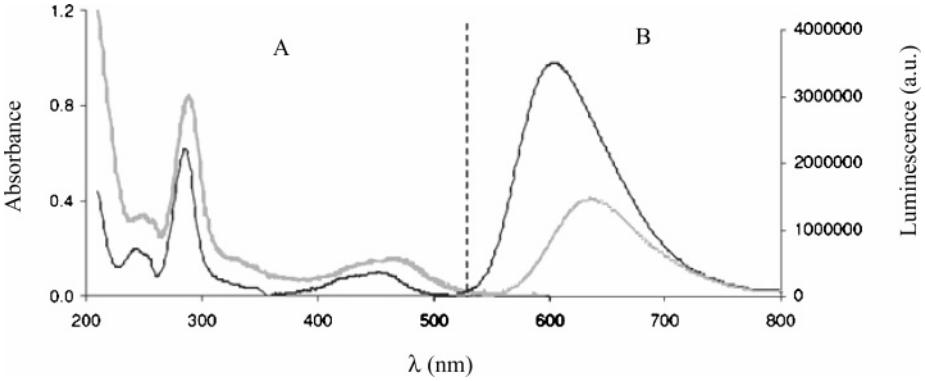

Figure 2. (A) Absorption and (B) emission (λ_{ex} = 455 nm) spectra of $[RuII(bpy)_3]^{2+}$ (black line) (6×10^{-5} M) and $[Ru(L_2)_2(L_1)]^{2+}$ (gray line) (5×10^{-5} M) in deoxygenated CH_3CN at 298 K.

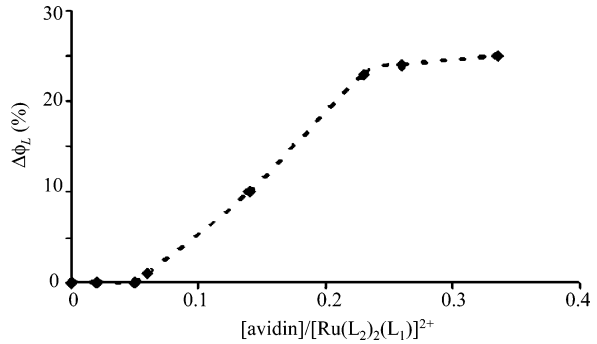

Figure 3. Percentage increase in the quantum yield luminescence of a $[Ru(L_2)_2(L_1)]^{2+}$ solution (1.7×10^{-5} M) in deoxygenated H_2O as a function of avidin concentration.

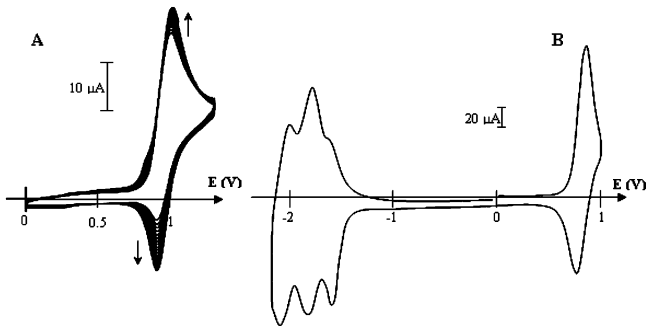

Figure 4. (A) Oxidative electropolymerization of $[Ru(L_2)_2(L_1)]^{2+}$ (10^{-3} M) in CH_3CN + 0.1 M TBAP, by repeated potential scans between 0 and 1.3 V at a platinum electrode. (B) Resulting modified electrode after transfer into clean electrolyte. Scan rate: 100 mV s^{-1}.

observed for $[Ru(bpy)_3]^{2+}$ solution. This suggests the specific binding of biotin moieties of the ruthenium complex to avidin. These observations are in accordance with previous results reported on luminescent biotinylated ruthenium phenanthroline and ruthenium polypyridine complexes.[28−30] The authors ascribe the luminescence enhancement of complexes in the presence of avidin to the hydrophobicity of biotin-binding sites of the protein that changes the local environment of the Ru complex upon binding interaction. The evolution of the quantum yield luminescence ($\Delta\phi_L$) as a function of $[avidin]/[Ru(L_2)_2(L_1)]^{2+}$ ratio shows that the luminescence stabilization occurs for $[avidin]/[Ru(L_2)_2(L_1)]^{2+}$ = 1/4 (Figure 3). This clearly indicates that 4 Ru complexes are bound to one avidin molecule. Because no additional luminescence increase is observed for a higher $[avidin]/[Ru(L_2)_2(L_1)]^{2+}$ ratio, it seems that only one biotin group per Ru can lead to an avidin association. Taking into account the steric hindrances generated by the avidin binding and the distance between both biotin moieties, it is more likely that one Ru center cannot act as a bridge between two avidin molecules.

Electrochemical Elaboration and Characterization of Poly Ru Films. Upon oxidative scanning, the electrochemical behavior of $[Ru(L_2)_2(L_1)]^{2+}$ complex (1 mM) in CH_3CN + 0.1 M TBAP depicted a poorly reversible peak system at 0.92 V corresponding to the irreversible oxidation of the pyrrole groups catalyzed by the $Ru^{III/II}$ redox couple (Figure 4A). The electropolymerization of $[Ru(L_2)_2(L_1)]^{2+}$ was thus carried out by repeated potential cycling over the range 0−1.3 V. The continuous increase in the intensity and reversibility of $Ru^{III/II}$ peak system clearly indicates the formation of a polymeric coating onto the electrode surface (Figure 4A). Although the high upper limit of the potential scanning (1.3 V) induces the overoxidation of the electrogenerated polypyrrole chains and hence the loss of their conductivity, the ruthenium(II) centers can act as a relay for the electropolymerization of pyrrole groups allowing a sustained growth of the polymeric film. Upon transfer of the resulting modified electrode into CH_3CN free of monomer, its cyclic voltammogram exhibits the reversible $Ru^{III/II}$ peak system in the positive region and three redox couples in the negative region due to the one-electron reduction of each bipyridyl ligand. This confirms the formation of a stable adherent polymer on the electrode surface (Figure 4B). Electropolymerization of $[Ru(L_2)_2(L_1)]^{2+}$ was also achieved by controlled-potential oxidation at 0.9 V. As expected, the apparent surface concentration of poly Ru (Γ, determined from the charge integrated under the $Ru^{III/II}$ peak system) increases with the increase in electropolymerization charge. In a typical experiment, a mean electropolymerization yield of 50% was determined by dividing the charge integrated for the oxidation of the polymerized Ru(II) complexes by the charge employed for the electropolymerization and multiplying by 9.3 that corresponds to 2.33 electrons per pyrrole group.[31]

The photophysical behavior of the biotinylated ruthenium complex under its polymerized form coated on an ITO surface is closely related to that of the monomer in solution. The UV−visible absorption spectrum exhibits a maximum at 468 nm attributed to the MLCT transition, and emission is detected with a maximum around 615 nm. The luminescence decay of the film can be fit by a monoexponential with a lifetime (85 ns)

(28) Slim, M.; Sleiman, H. F. *Bioconjugate Chem.* **2004**, *15*, 949.
(29) Hofmeier, H.; Pahnke, J.; Weidl, C. H.; Schubert, U. S. *Biomacromolecules* **2004**, *5*, 2055.
(30) Lo, K. K.-W.; Lee, T. K.-M. *Inorg. Chem.* **2004**, *17*, 5275.

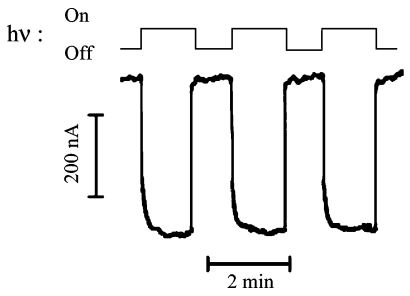

Figure 5. Time-based photocurrent response of polypyrrole ruthenium electrode ($\Gamma = 2.3 \times 10^{-8}$ mol cm^{-2}) in the presence of Co(III) (15 mM) in 0.1 M acetate buffer (pH 5) as the excitation light turned on and off.

shorter than that of the monomer. This rapid relaxation of the ^{3}MLCT state can be attributed to a partial inhibition by oxygen and to a self-quenching by the Ru(II) complexes, which are spatially close in the polymer film. Nevertheless, the lifetime of the excited state of Ru(II) in the polymer film remains long enough to be engaged in a bimolecular reaction with an external electron acceptor (or donor).

Photoelectrochemical Analysis of Polymeric Film. Because Ru complexes were widely used as photosensitizer, the photoelectrochemical properties of the polypyrrole−ruthenium(II) film were examined under illumination by white light in the presence of Co(III) (15 mM) as oxidative quencher. Figure 5 shows a typical response of a poly$[Ru(L_2)_2(L_1)]^{2+}$/Pt electrode ($\Gamma = 2.3 \times 10^{-8}$ mol cm^{-2}) as the excitation light was turned on and off. The steady-state value of the cathodic photocurrent was quickly reached (1.8 μA cm^{-2}) and was stable with time. The irradiation process was repeated 20 times over 50 min, providing reproducible photocurrent responses without noticeable decrease in their intensity. This demonstrates the repeatability of the photoelectrode response (RSD $\approx$ 2%) and hence the mechanical and photophysical stability of the film. It should be noted that the photolysis of the poly Ru film in the absence of Co(III) or the irradiation of a bare platinum electrode in the presence of Co(III) did not cause any photocurrent. Because it is well-known that Co(III) is a good quencher for excited $[Ru(bpy)_3]^{2+}$ in aqueous solution, the photoelectrochemical response corresponds to the irreversible oxidative quenching of the excited state of the polymerized Ru(II) centers by Co(III) into Ru(III).[32] The latter was subsequently reduced into the initial Ru(II) by the electrode held at 0.5 V, thus creating a photoelectrochemical cycle leading to a cathodic photocurrent. Scheme 1 represents the mechanism relative to the photocurrent production.

The intensity of photocurrent "I_{ph}" increases with increased concentration of added quencher and reached maximum for Co(III) = 8 mM, while a weak decrease was observed for higher concentrations (Figure 6). This phenomenon may be ascribed to the absorbance of saturated quencher solution at 15 mM, decreasing thus the irradiation intensity and the efficiency of excited ruthenium center formation. Figure 7 shows the evolution of the steady-state photocurrent I_{ph} as a function of the film thickness in the presence of an identical amount of Co(III) (15 mM). I_{ph} increases continuously with film thickness, highlighting the fact that the irradiation process and the

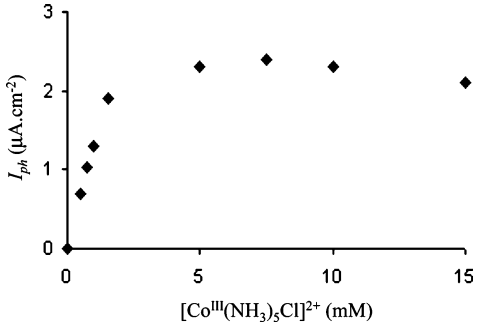

Figure 6. Plot of the steady-state photocurrent response of a poly Ru electrode ($\Gamma = 2 \times 10^{-8}$ mol cm^{-2}) in 0.1 M acetate buffer (pH 5) as function of Co(III) concentration. Applied potential 0.5 V vs SCE.

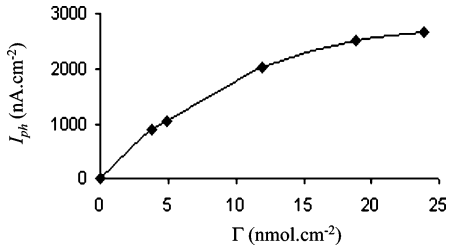

Figure 7. Evolution of the steady-state photocurrents as a function of poly Ru film thickness in the presence of Co(III) (15 mM). Experimental conditions are as in Figure 6.

Scheme 1. Representation of the Mechanism of Cathodic Current Generation from a Polypyrrole Ruthenium(II) Film under Irradiation in the Presence of an Oxidative Quencher (Co(III))

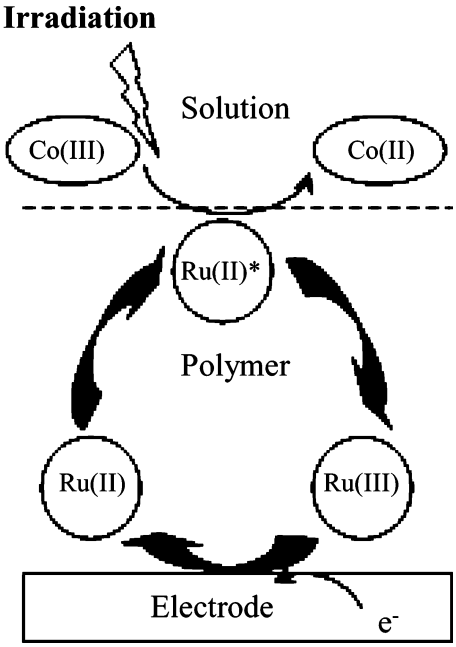

subsequent quenching by the cobalt complex take place at the film/solution interface but also within the whole structure of the film.

Avidin-Binding Properties of Polymeric Film. The ability to immobilize avidin on the poly Ru film and hence the availability of polymerized biotin groups has been examined through the use of avidin labeled alkaline phosphatase (AP). A poly Ru electrode was soaked in AP solution (0.5 mg mL^{-1}) to elaborate an enzyme monolayer by formation of avidin−biotin interactions. Because of the phosphohydrolytic activity of AP, the enzymatic activity of the resulting electrode was determined

(31) Cosnier, S.; Deronzier, A.; Roland, J. F. *J. Electroanal. Chem.* **1990**, *285*, 133.
(32) Gafney, H. D.; Adamson, A. W. *J. Am. Chem. Soc.* **1972**, *94*, 8238.

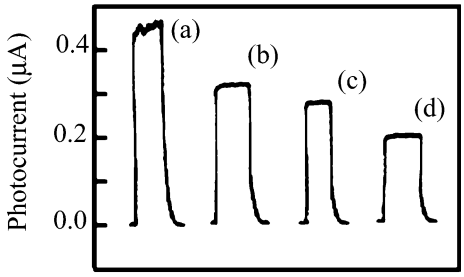

Figure 8. Photocurrent response of a modified electrode in the presence of Co(III) (15 mM) in 0.1 M acetate buffer (pH 5), (a) before and (b) after avidin immobilization, (c) after cholera toxin B anchoring, and (d) after incubation with the corresponding antibody (anti CT, 0.5 mg/mL).

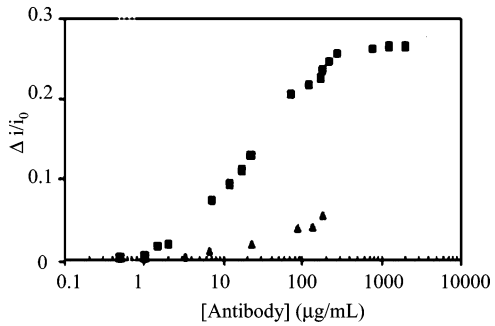

Figure 9. Calibration curves for photoelectrochemical immunosensors with antibodies ranging from 0 to 200 μg mL^{-1}: (A) anti CT antibody (■), (B) noncomplementary IgG antibody (▲).

by following at 410 nm the absorbance of *p*-nitrophenol produced from the substrate *p*-nitrophenyl phosphate. Its comparison with the activity of free enzyme in solution allows estimation of a surface coverage of AP to 640 ng cm^{-2}. Taking into account that the theoretical maximum surface coverage for a compact enzyme monolayer was estimated to 3.53×10^{-12} mol cm^{-2} or 522 ng cm^{-2}, the AP coverage corresponds to the formation of 1.2 compact monolayer onto the polymer film.[33] This illustrates that the polymerized biotin groups can penetrate the binding site of avidin, providing an efficient immobilization of the avidin-conjugated enzyme. To validate the specific interaction between avidin and biotin groups, a control experiment was carried out with a native alkaline phosphatase. After the incubation step with a poly Ru film, no enzymatic activity was spectrometrically detected for the resulting electrode, corroborating thus the role of avidin−biotin interaction in the enzyme immobilization process.

Photoelectrochemical Immunosensor. Increased attention has been given recently to direct label-free electrochemical detection schemes of hybridizations or immunoreactions, in which the recognition event triggers a change in the intrinsic electrochemical properties of the interface. Therefore, the possibility to exploit the photoelectrochemical properties of the biotinylated poly Ru film for the transduction of surface molecular recognition process without labeling of the target was investigated for the detection of anti-cholera toxin antibody (anti CT) as model system. The development of new vaccines against cholera for epidemiological reasons indeed requires analytical tools for the detection of the corresponding antibody that reflects the immunization. For this purpose, the biotinylated film was applied to the anchoring of avidin and subsequent binding of the biotinylated probe, cholera toxin B subunit biotin-labeled (CT), via avidin−biotin interactions, thus providing an immunosensing surface able to bind the corresponding antibody. The specific buildup of three protein layers (avidin and immunogenic material) was carried out on the poly Ru films ($\Gamma = 2.5 \times 10^{-8}$ mol cm^{-2}). As expected, the successive binding of avidin and biotinylated toxin on the biotinylated film induces a marked decrease in the photocurrent response generated in the presence of Co(III) (Figure 8). Such a decrease in photoelectrochemical current intensity was ascribed to the increase in steric hindrances toward the diffusion of quencher molecules to the underlying poly Ru film with the increase in protein layers, thus lowering the amount of photogenerated Ru(III) center. Although the anti CT layer constitutes the third protein layer, its formation has also a marked influence on the photocurrent intensity. A 28% intensity decrease was recorded, thus reflecting the antibody anchoring. Control experiments carried out with avidin-conjugated poly Ru films incubated with anti CT or successively incubated with regular toxin and anti CT indicated no change in photocurrent intensity. This clearly demonstrates that the preceding photocurrent decrease reflected specifically an immunoreaction instead of a nonspecific binding of proteins on the immobilized avidin layer.

This photocurrent variation was thus exploited for detecting directly immunoreactions without additional labeling step of the target. A calibration curve for the detection of antibody was elaborated by recording, for each anti CT concentration in the range 0−200 μg mL^{-1}, the photocurrent decrease observed for a modified electrode. It should be noted that a new immunosensor was used for each antibody concentration. The normalized photocurrent response gradually increases with increasing antibody concentrations and ultimately leveled off for concentrations higher than 100 μg mL^{-1}, the detection limit being 0.5 μg mL^{-1} (Figure 9A). The selectivity of the photoelectrochemical immunosensor was also investigated by following the change in the photoelectrochemical current induced by different concentrations of noncomplementary antibody IgG (Figure 9B). It clearly appears that the normalized photocurrent response due to the nonspecific adsorption of immunoglobulin was markedly lower than those induced by the specific binding of anti CT antibody.

Conclusion

We have presented herein a new photoelectrochemical strategy of immunoreaction detection, allowing the direct quantification of the target without a labeling step. The novelty consisted in the electropolymerization of a biotinylated poly(pyrrole-ruthenium) film as a photosensitive and anchoring polymeric layer. It is expected that this precursor polymer will be useful for the fabrication of label-free affinity sensors.

Acknowledgment. We thank the Commission of the European Communities Research Directorate for their support under ELISHA project contract No. NMP-A-CT-2003-505485-1.

JA062729Z

(33) Mousty, C.; Bergamasco, J.-L.; Wessel, R.; Perrot, H.; Cosnier, S. *Anal. Chem.* **2001**, *73*, 2890.